

Structural Design Principles for Hybrid Cadmium Thiocyanate-Halides Containing Bulky Organic Cations

Alexander Milder and Patrick M. Woodward

*Department of Chemistry and Biochemistry, The Ohio State University, Columbus, Ohio 43210,
United States*

Corresponding Author: PMW: woodward.55@osu.edu

Supplementary Information

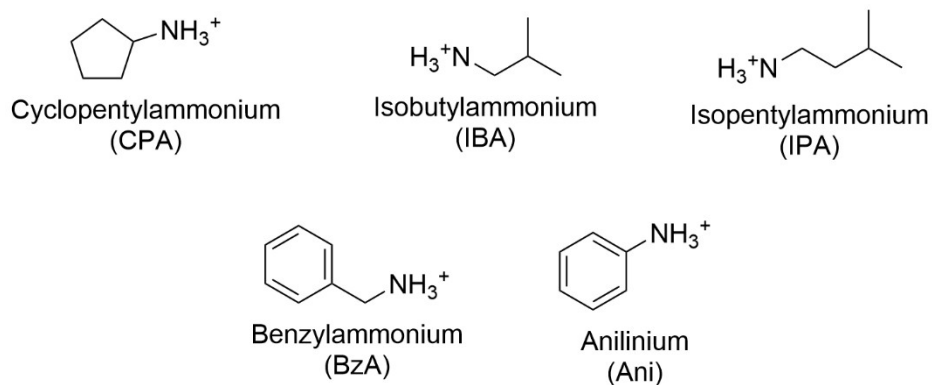


Figure S1: Structures and abbreviations used for the new compounds reported in this work

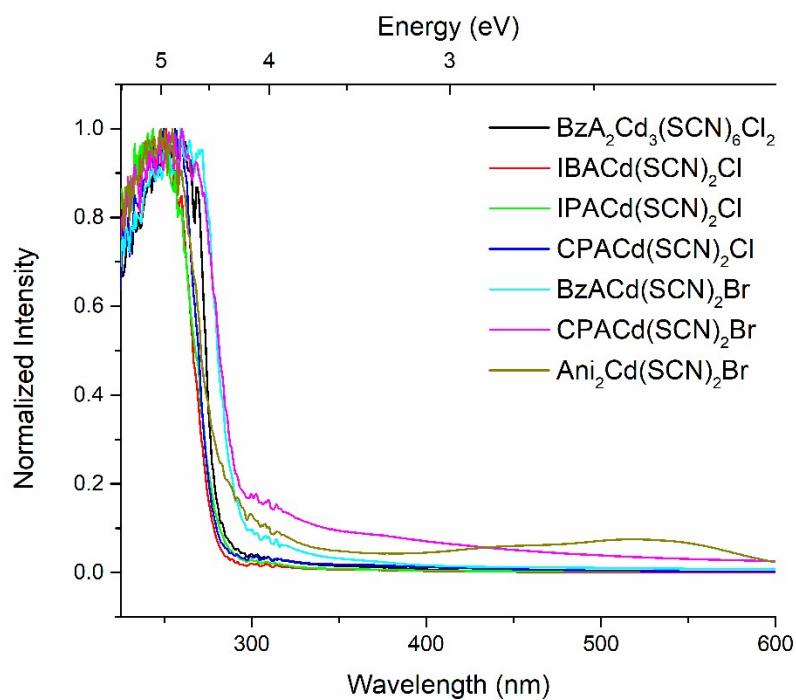


Figure S2: DRS data for all new compounds reported in this work. The vertical axis represents Kubelka-Munk transformed pseudo-absorbance, normalized by dividing by the maximum intensity of each trace.

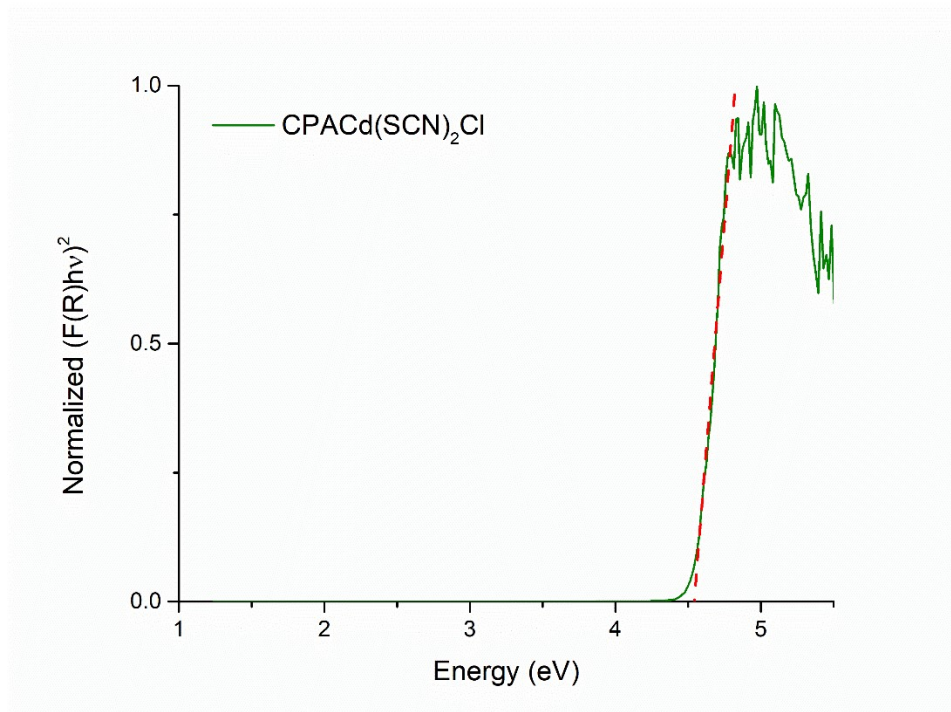


Figure S3: Tauc plot of compound **1** showing measured direct band gap of 4.54 eV. The green trace is the square of the Kubelka-Munk transformed pseudo absorbance, $F(R)$, multiplied by the photon energy, $h\nu$. We assume a direct band gap so this quantity is squared to complete the Tauc plot. The red dashed lines show the extrapolated fit to the linear portion of this plot, which is used to determine the band gap.

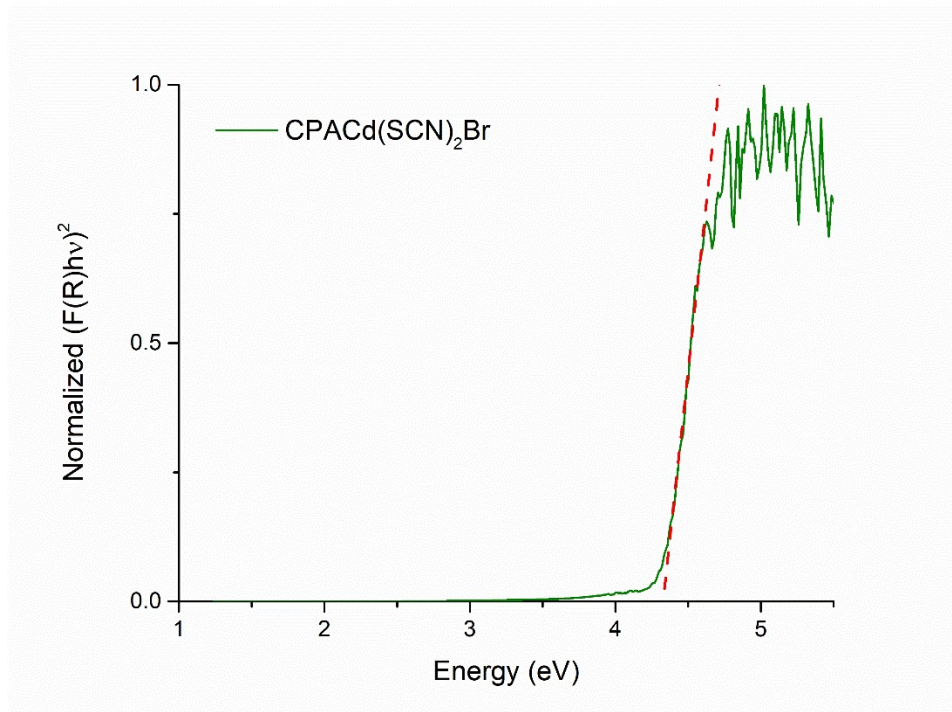


Figure S4: Tauc plot of compound **2** showing measured direct band gap of 4.33 eV. The green trace is the square of the Kubelka-Munk transformed pseudo absorbance, $F(R)$, multiplied by the photon energy, $h\nu$. We assume a direct band gap so this quantity is squared to complete the Tauc plot. The red dashed lines show the extrapolated fit to the linear portion of this plot, which is used to determine the band gap.

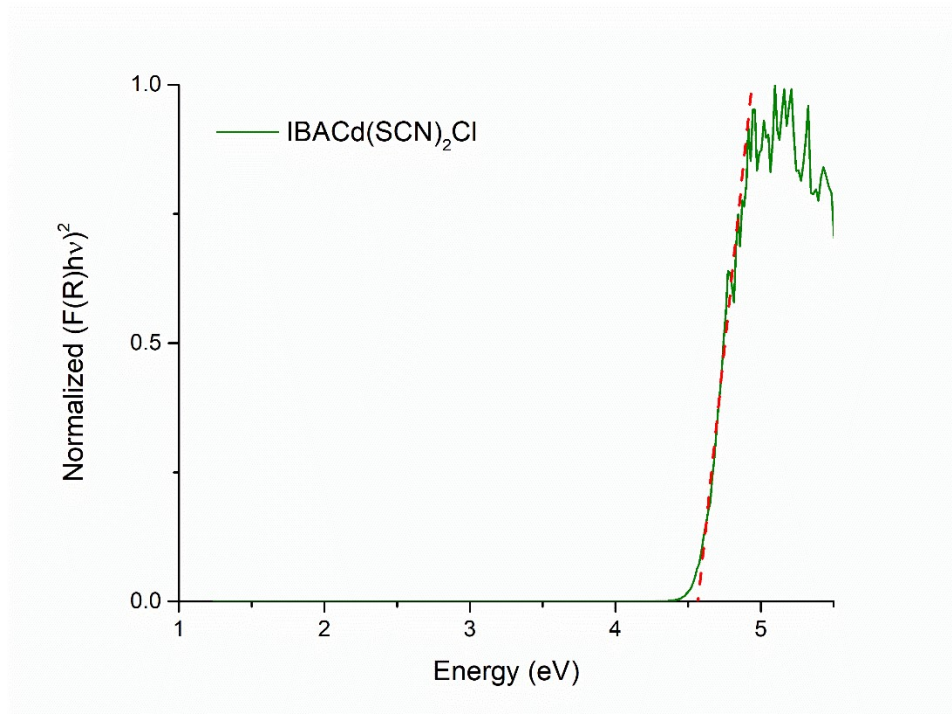


Figure S5: Tauc plot of compound **3** showing measured direct band gap of 4.57 eV. The green trace is the square of the Kubelka-Munk transformed pseudo absorbance, $F(R)$, multiplied by the photon energy, $h\nu$. We assume a direct band gap so this quantity is squared to complete the Tauc plot. The red dashed lines show the extrapolated fit to the linear portion of this plot, which is used to determine the band gap.

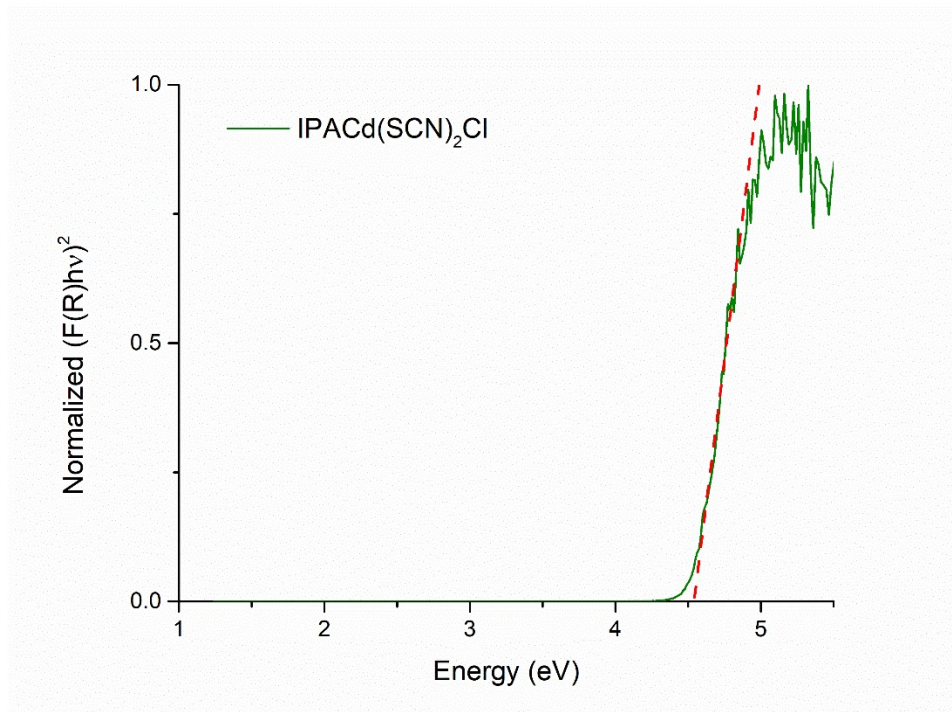


Figure S6: Tauc plot of compound **4** showing measured direct band gap of 4.54 eV. The green trace is the square of the Kubelka-Munk transformed pseudo absorbance, $F(R)$, multiplied by the photon energy, $h\nu$. We assume a direct band gap so this quantity is squared to complete the Tauc plot. The red dashed lines show the extrapolated fit to the linear portion of this plot, which is used to determine the band gap.

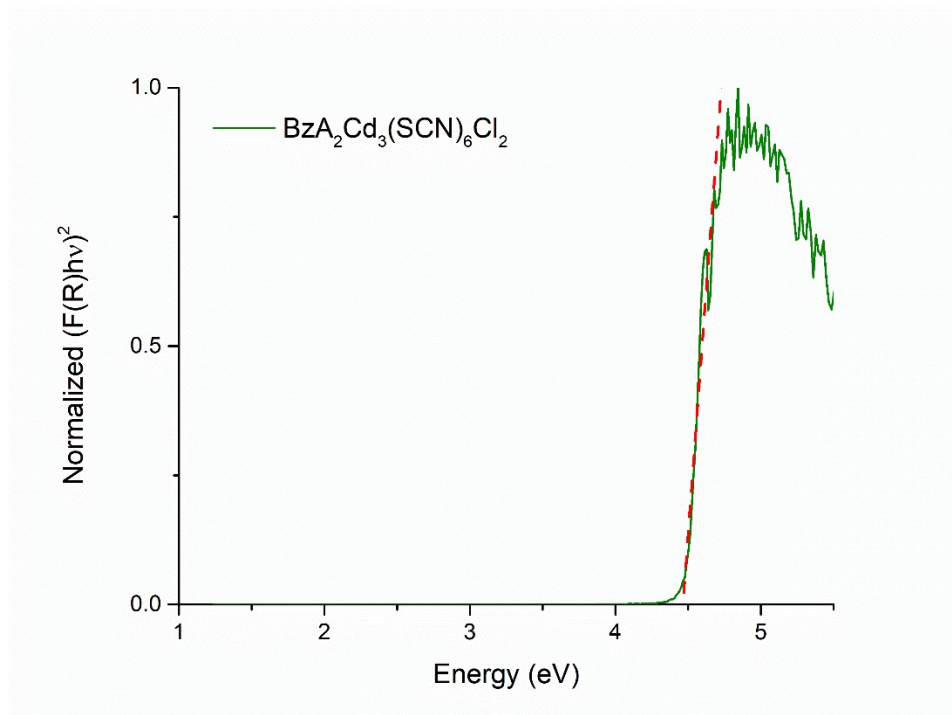


Figure S7: Tauc plot of compound **5** showing measured direct band gap of 4.46 eV. The green trace is the square of the Kubelka-Munk transformed pseudo absorbance, $F(R)$, multiplied by the photon energy, $h\nu$. We assume a direct band gap so this quantity is squared to complete the Tauc plot. The red dashed lines show the extrapolated fit to the linear portion of this plot, which is used to determine the band gap.

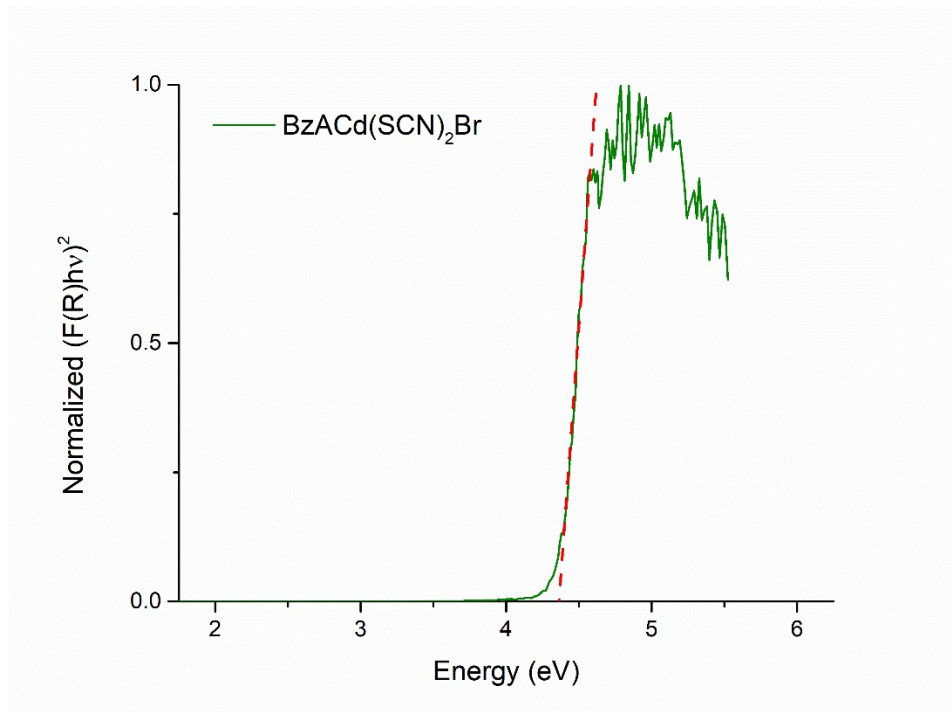


Figure S8: Tauc plot of compound **6** showing measured direct band gap of 4.36 eV. The green trace is the square of the Kubelka-Munk transformed pseudo absorbance, $F(R)$, multiplied by the photon energy, $h\nu$. We assume a direct band gap so this quantity is squared to complete the Tauc plot. The red dashed lines show the extrapolated fit to the linear portion of this plot, which is used to determine the band gap.

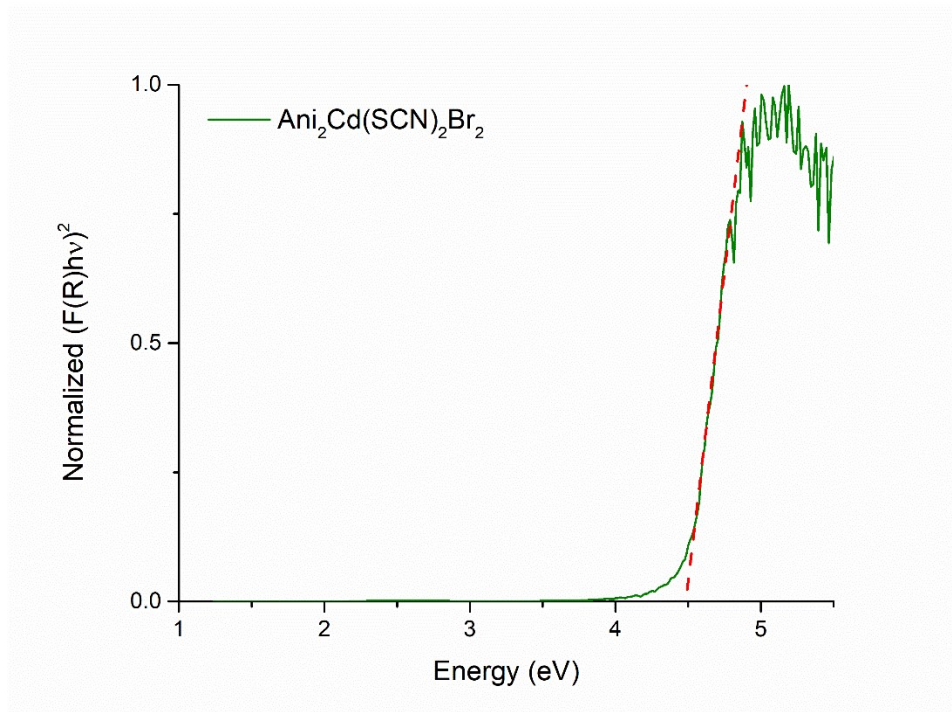


Figure S9: Tauc plot of compound **7** showing measured direct band gap of 4.48 eV. The green trace is the square of the Kubelka-Munk transformed pseudo absorbance, $F(R)$, multiplied by the photon energy, $h\nu$. We assume a direct band gap so this quantity is squared to complete the Tauc plot. The red dashed lines show the extrapolated fit to the linear portion of this plot, which is used to determine the band gap.

Figures S10-S16: Representative powder X-ray diffraction data and Pawley refinements for ground crystals of compounds **1-7**. Data was collected on either a Bruker D8 Advance powder diffractometer equipped with a monochromated Cu sealed tube source or a Rigaku Miniflex I powder diffractometer with a non-monochromated Cu source as noted.

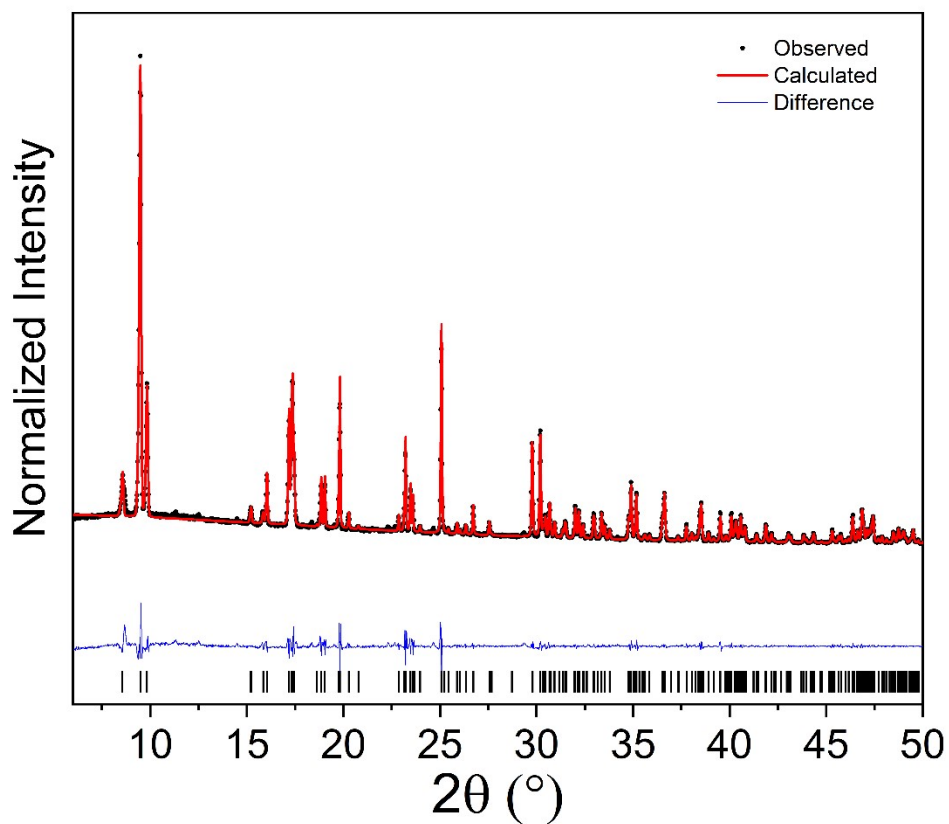


Figure S10: PXRD and Pawley refinement of compound **1** from data collected on the Bruker D8 instrument.

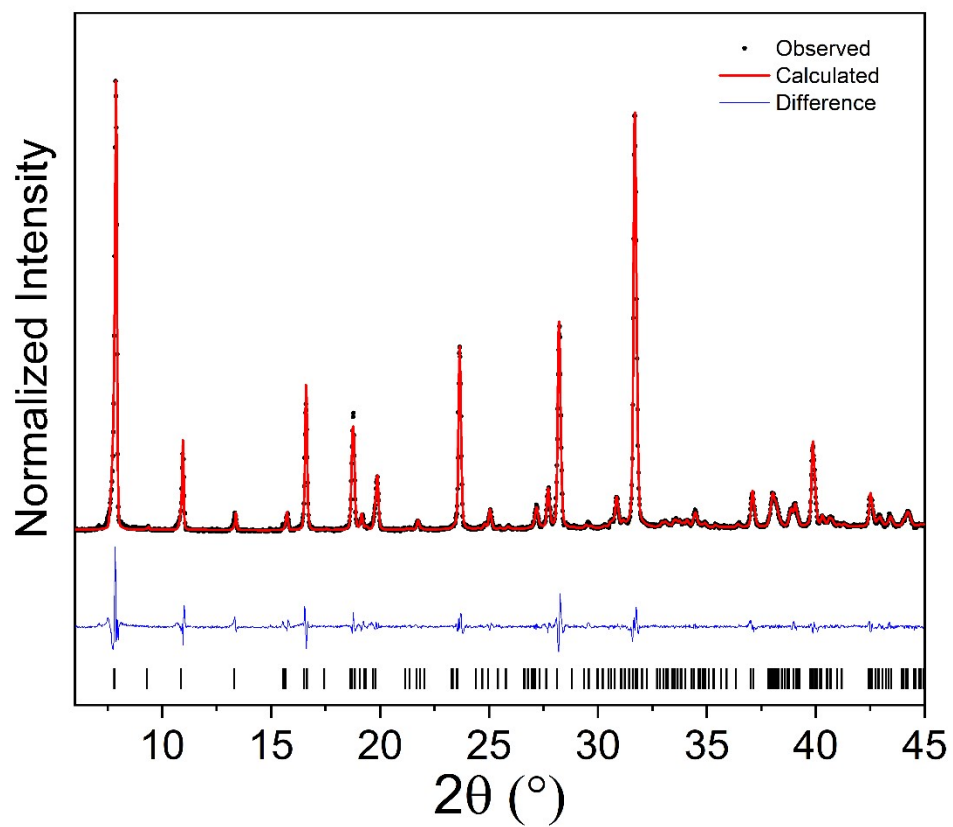


Figure S11: PXRD and Pawley refinement of compound **2** from data collected on the Rigaku Miniflex I instrument.

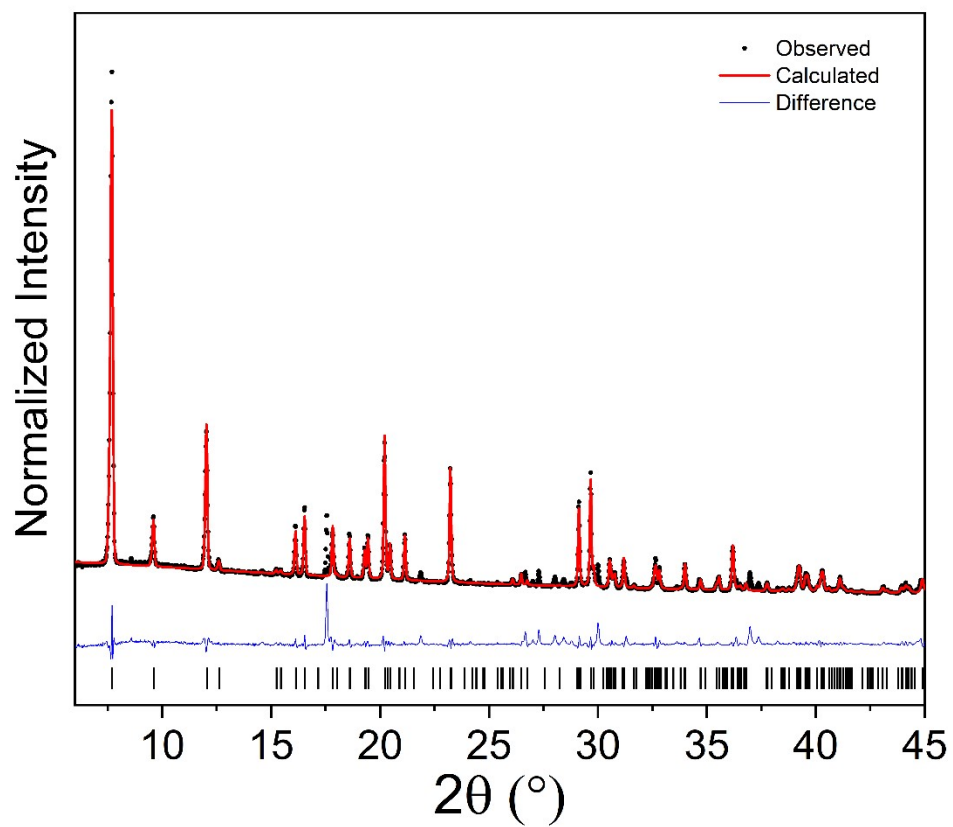


Figure S12: PXRD and Pawley refinement of compound **3** from data collected on the Bruker D8 instrument.

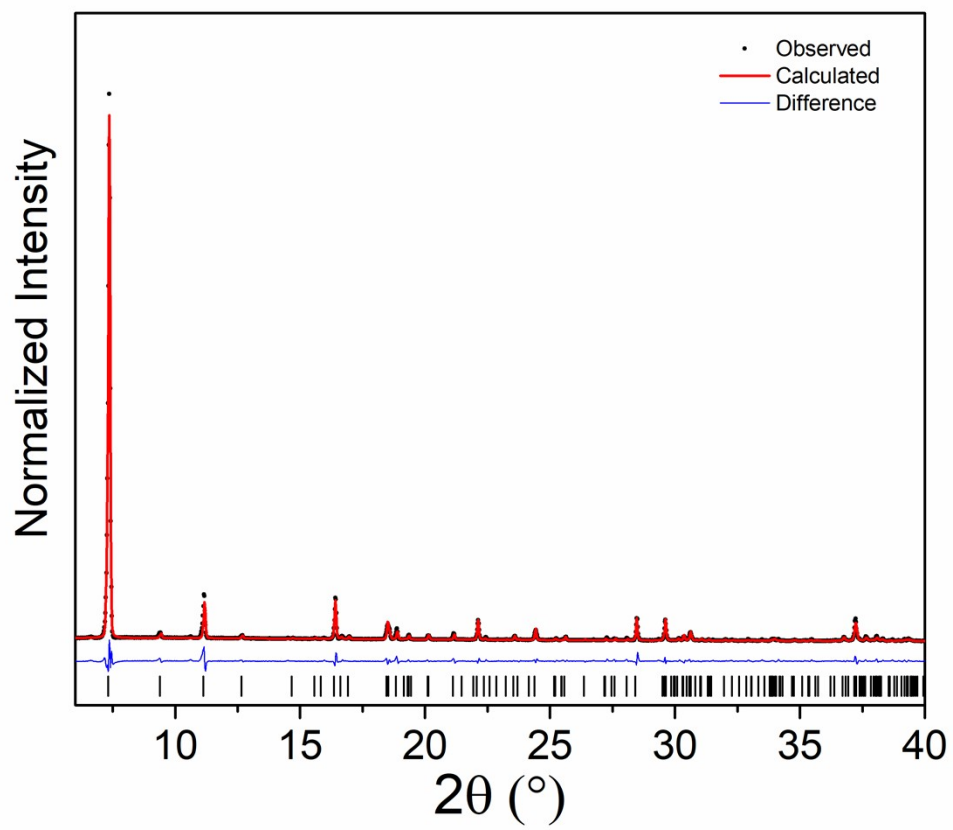


Figure S13: PXRD and Pawley refinement of compound **4** from data collected on the Bruker D8 instrument.

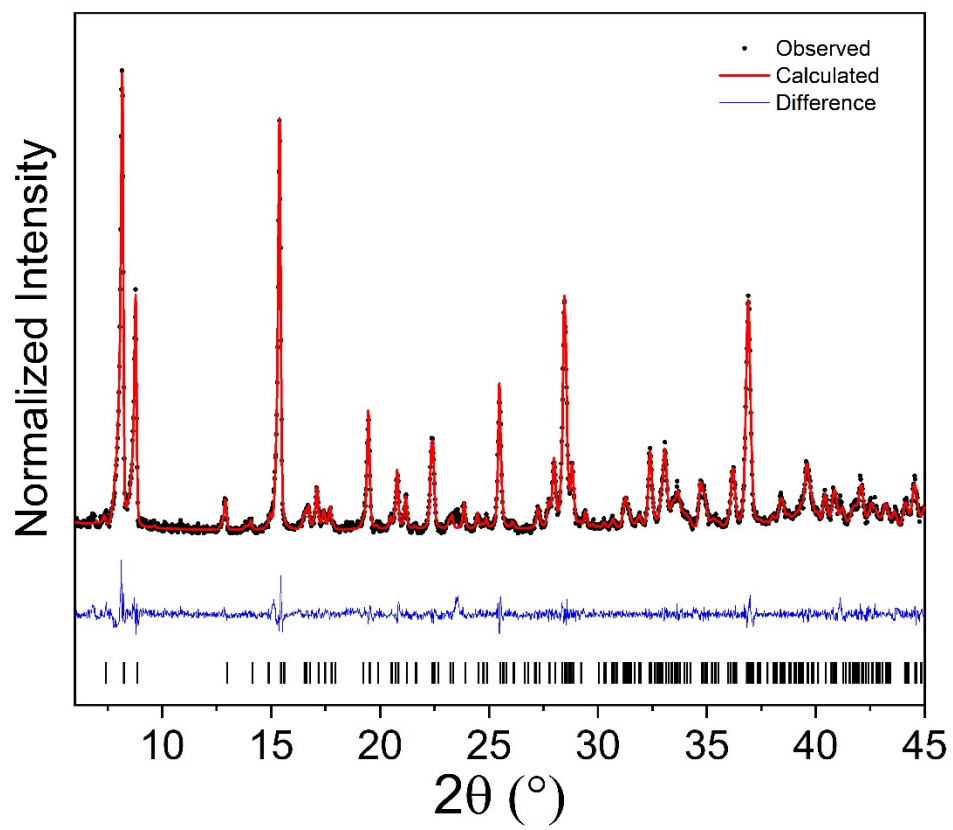


Figure S14: PXRD and Pawley refinement of compound **5** from data collected on the Bruker D8 instrument.

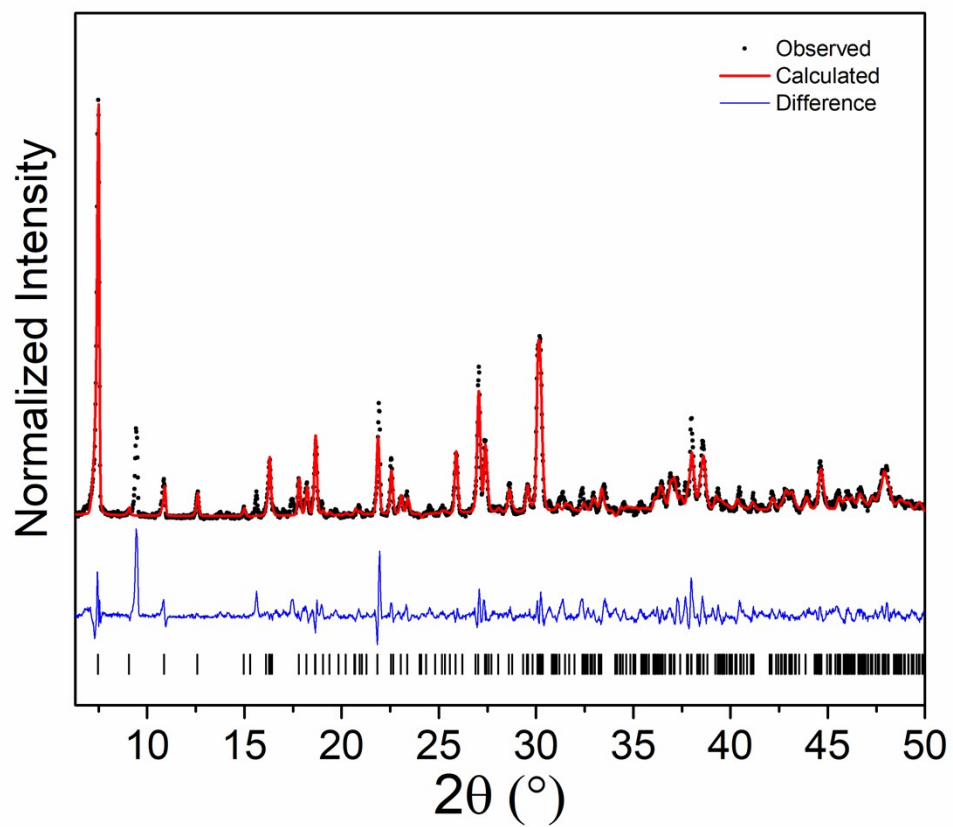


Figure S15: PXRd and Pawley refinement of compound **6** from data collected on the Rigaku Miniflex I instrument.

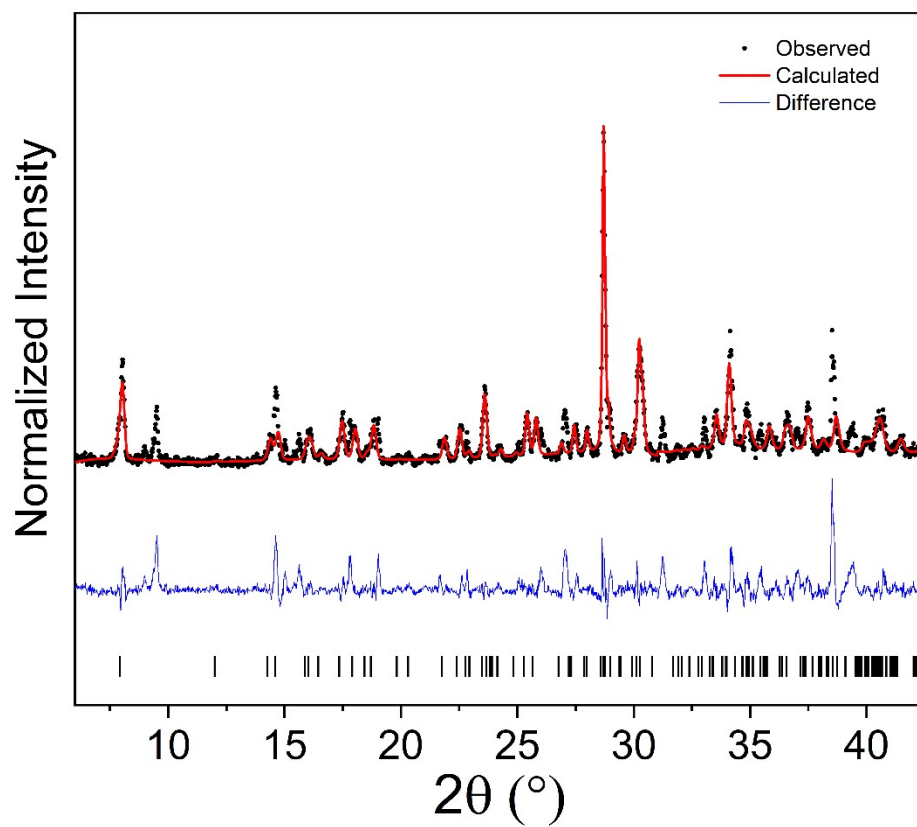


Figure S16: PXRd and Pawley refinement of compound 7 from data collected on the Rigaku Miniflex I instrument.

Table S1: Lattice parameters and refinement indicators for compounds 1–4

Composition	CPACd(SCN) ₂ Cl	CPACd(SCN) ₂ Br	IBACd(SCN) ₂ Cl	IPACd(SCN) ₂ Cl
<i>T</i> (K)	298	298	100	100
Space Group	<i>P</i> $\bar{1}$	<i>P</i> $\bar{1}$	<i>P</i> $\bar{1}$	<i>P</i> $\bar{1}$
<i>a</i> (Å)	5.9082(4)	5.9164(6)	5.9664(3)	5.8644(2)
<i>b</i> (Å)	10.2084(8)	9.8218(12)	9.2609(4)	9.7409(4)
<i>c</i> (Å)	11.4671(8)	11.8747(15)	11.1509(5)	12.1164(5)
α (°)	113.822(2)	99.211(4)	87.173(2)	79.4470(10)
β (°)	99.670(2)	103.298(4)	83.075(2)	78.1680(10)
γ (°)	90.293(2)	98.195(4)	79.6580(10)	79.1370(10)
<i>V</i> (Å ³)	621.66(8)	651.22(13)	601.46(5)	657.74(4)
<i>Z</i>	2	2	2	2
<i>R</i> ₁ / <i>wR</i> ₂ (%)	3.77/7.43	4.59/8.56	2.32/4.75	1.75/4.36
Density (g/cm ³)	1.871	2.013	1.867	1.778
Absorption Coefficient (mm ⁻¹)	2.274	5.034	2.347	2.150
F(000)	344	380	332	348
θ Range for Data Collection (°)	3.500–28.385	3.058–28.375	3.494–28.356	3.595–28.350
Index Ranges	$-7 \leq h \leq 7$ $-13 \leq k \leq 13$ $-15 \leq l \leq 15$	$-7 \leq h \leq 7$ $-13 \leq k \leq 13$ $-15 \leq l \leq 15$	$-7 \leq h \leq 7$ $-12 \leq k \leq 12$ $-14 \leq l \leq 14$	$-7 \leq h \leq 7$ $-12 \leq k \leq 12$ $-16 \leq l \leq 16$
Reflections collected	35761	39452	32292	31508
Independent Reflections	3107	3249	2989	3219
Parameters Refined	128	128	121	172
Completeness to 50.5° (%)	99.9	99.9	99.8	97.5
Goodness of fit	1.025	1.005	1.137	1.105
Largest Difference Peak and Hole	0.5/–0.4	0.5/–0.6	0.4/–0.4	0.6/–0.5

Table S2: Lattice parameters and refinement indicators for compounds 4-6

Composition	BzA ₂ Cd ₃ (SCN) ₆ Cl ₂	BzACd(SCN) ₂ Br	Ani ₂ Cd(SCN) ₂ Br ₂
<i>T</i> (K)	298	298	298
Space Group	<i>P</i> 2 ₁ / <i>n</i>	<i>P</i> $\bar{1}$	<i>C</i> 2/ <i>c</i>
<i>a</i> (Å)	12.7917(17)	5.8458(3)	22.100(2)
<i>b</i> (Å)	5.8894(7)	10.1305(6)	7.8037(7)
<i>c</i> (Å)	21.896(3)	12.1382(6)	11.0731(8)
α (°)	90	79.520(2)	90
β (°)	101.592(4)	80.742(2)	94.037(5)
γ (°)	90	76.902(2)	90
<i>V</i> (Å ³)	1615.9(4)	683.06(6)	1905.0(3)
<i>Z</i>	2	2	4
<i>R</i> ₁ / <i>wR</i> ₂ (%)	2.96/7.72	3.30/6.65	1.92/4.82
Density (g/cm ³)	2.000	2.026	2.011
Absorption Coefficient (mm ⁻¹)	2.536	4.806	5.563
F(000)	940	400	1112
θ Range for Data Collection (°)	2.983-26.594	2.900-28.401	3.689-28.411
Index Ranges	-16 ≤ <i>h</i> ≤ 16 -7 ≤ <i>k</i> ≤ 7 -27 ≤ <i>l</i> ≤ 27	-7 ≤ <i>h</i> ≤ 7 -13 ≤ <i>k</i> ≤ 13 -16 ≤ <i>l</i> ≤ 16	-7 ≤ <i>h</i> ≤ 7 -13 ≤ <i>k</i> ≤ 13 -15 ≤ <i>l</i> ≤ 15
Reflections collected	56748	23247	53331
Independent Reflections	3379	3411	2386
Parameters Refined	179	146	106
Completeness to 50.5° (%)	99.7	99.9	99.8
Goodness of fit	1.067	1.002	1.047
Largest Difference Peak and Hole	0.5/-0.5	0.4/-0.5	0.6/-1.0

Table S3: Band gaps determined from DRS using the Tauc method and the DFT calculated band structures

	Direct E_g from DRS (eV)	Direct E_g from DFT (eV)	Indirect E_g from DFT (eV)
CPACd(SCN) ₂ Cl	4.54	3.79	3.74
CPACd(SCN) ₂ Br	4.33	3.63	3.53
IBACd(SCN) ₂ Cl	4.57	---	---
IPACd(SCN) ₂ Cl	4.54	---	---
BzA ₂ Cd ₃ (SCN) ₆ Cl ₂	4.46	---	---
BzACd(SCN) ₂ Br	4.36	---	---
Ani ₂ Cd(SCN) ₂ Br ₂	4.48	---	---